

Static Hopfions in the extended Skyrme-Faddeev model

L. A. Ferreira^{a,*}, Nobuyuki Sawado^{a,b,†} and Kouichi Toda^{a,c,‡}

^a*Instituto de Física de São Carlos; IFSC/USP, Universidade de São Paulo - USP,
Caixa Postal 369, CEP 13560-970, São Carlos-SP, Brazil*

^b*Department of Physics, Tokyo University of Science, Noda, Chiba 278-8510, Japan*

^c*Department of Mathematical Physics, Toyama Prefectural University,
Kurokawa 5180, Imizu, Toyama, 939-0398, Japan*

(Dated: June 2, 2018)

We construct static soliton solutions with non-zero Hopf topological charges to a theory which is an extension of the Skyrme-Faddeev model by the addition of a further quartic term in derivatives. We use an axially symmetric ansatz based on toroidal coordinates, and solve the resulting two coupled non-linear partial differential equations in two variables by a successive over-relaxation (SOR) method. We construct numerical solutions with Hopf charge up to four, and calculate their analytical behavior in some limiting cases. The solutions present an interesting behavior under the changes of a special combination of the coupling constants of the quartic terms. Their energies and sizes tend to zero as that combination approaches a particular special value. We calculate the equivalent of the Vakulenko and Kapitanskii energy bound for the theory and find that it vanishes at that same special value of the coupling constants. In addition, the model presents an integrable sector with an infinite number of local conserved currents which apparently are not related to symmetries of the action. In the intersection of those two special sectors the theory possesses exact vortex solutions (static and time dependent) which were constructed in a previous paper by one of the authors. It is believed that such model describes some aspects of the low energy limit of the pure $SU(2)$ Yang-Mills theory, and our results may be important in identifying important structures in that strong coupling regime.

I. INTRODUCTION

We construct static soliton solutions, carrying non-trivial Hopf topological charges, for a field theory that has found interesting applications in many areas of Physics. It is a $(3+1)$ -dimensional Lorentz invariant field theory for a triplet of scalar fields \vec{n} , living on the two-sphere S^2 , $\vec{n}^2 = 1$, and defined by the Lagrangian density

$$\mathcal{L} = M^2 \partial_\mu \vec{n} \cdot \partial^\mu \vec{n} - \frac{1}{e^2} (\partial_\mu \vec{n} \wedge \partial_\nu \vec{n})^2 + \frac{\beta}{2} (\partial_\mu \vec{n} \cdot \partial^\mu \vec{n})^2 \quad (1)$$

where the coupling constants e^2 and β are dimensionless, and M has dimension of mass. The first two terms correspond to the so-called Skyrme-Faddeev (SF) model [1], which was proposed long ago following Skyrme's idea [2], as the generalization to $3+1$ dimensions of the CP^1 model in $2+1$ dimensions [3]. The interest in the SF model has grown considerably in recent years since the first numerical knotted soliton solutions were constructed [4, 5, 6, 7, 8], as well as vortex type solutions [9, 10]. It has also found applications in Bose-Einstein condensates [11], superconductors [12, 13] and in the Weinberg-Salam model [14]. In addition, it has been conjectured by Faddeev and Niemi [15] that the SF model describes the low energy (strong coupling) regime of the pure $SU(2)$ Yang-Mills theory. That was based on the so-called Cho-Faddeev-Niemi-Shabanov decomposition [15, 16, 17, 18] of the $SU(2)$ Yang-Mills field \vec{A}_μ , where its six physical degrees of freedom are encoded into a triplet of scalars \vec{n} ($\vec{n}^2 = 1$), a massless $U(1)$ gauge field, and two real scalar fields. The motivation for such decomposition originates from the fact that the triplet \vec{n} can be used as an order parameter for a condensate of Wu-Yang monopoles, which classical solution can then be written as $\vec{A}_0 = 0$, $\vec{A}_i = \partial_i \vec{n} \wedge \vec{n}$, $i = 1, 2, 3$, with \vec{n} corresponding to the hedgehog configuration $\vec{n} = \vec{x}/r$.

The conjecture of Faddeev and Niemi requires non-perturbative calculations to be proved or disproved and so the discussions in the literature have been quite controversial. Lattice field theory simulations have discouraged its validity [19], and recently Faddeev himself has proposed some modifications for it [20]. Gies [21] has calculated the one-loop Wilsonian effective action for the $SU(2)$ Yang-Mills theory, using the Cho-Faddeev-Niemi-Shabanov decomposition,

*Electronic address: laf@ifsc.usp.br

†Electronic address: sawado@ph.noda.tus.ac.jp

‡Electronic address: kouichi@yukawa.kyoto-u.ac.jp

and found agreements with the conjecture provided the SF model is modified by additional quartic terms in derivatives of the \vec{n} field. In fact, Gies obtained an effective action which up to first derivatives of \vec{n} is of the form (1). Similar results were obtained in [22] for the connection between the low energy Yang-Mills dynamics and modifications of Skyrme-Faddeev model using the Gaussian approximation of the vacuum wave functional. In this sense the extended version of the Skyrme-Faddeev model given by the theory (1) deserves some attention. Like the SF model it presents the internal $O(3)$ symmetry and admit solutions with topology given by the Hopf map $S^3 \rightarrow S^2$. The main difference is the fact that (1) contains quartic terms in time derivatives and so its canonical Hamiltonian is not positive definite when hard modes of the \vec{n} field are allowed. Indeed, that is a feature of many low energy effective theories.

The theory (1) has many interesting aspects which deserves attention as we now explain. It has two sectors where the static energy density is positive definite and one of them intersects with an integrable sub-sector of (1) with an infinite number of conservation laws. In a Minkowski space-time the static Hamiltonian associated to (1) is

$$\mathcal{H}_{\text{static}} = M^2 \partial_i \vec{n} \cdot \partial_i \vec{n} + \frac{1}{e^2} (\partial_i \vec{n} \wedge \partial_j \vec{n})^2 - \frac{\beta}{2} (\partial_i \vec{n} \cdot \partial_i \vec{n})^2 \quad (2)$$

with $i, j = 1, 2, 3$. Therefore, it is positive definite for $M^2 > 0$, $e^2 > 0$ and $\beta < 0$. That is the sector explored in [23], and where static soliton solutions with non-trivial Hopf topological charges were constructed.

One can now stereographic project S^2 on a plane and work with a complex scalar field u related to the triplet \vec{n} by

$$\vec{n} = \frac{1}{1 + |u|^2} (u + u^*, -i(u - u^*), |u|^2 - 1) \quad (3)$$

It then follows that

$$\begin{aligned} \vec{n} \cdot (\partial_\mu \vec{n} \wedge \partial_\nu \vec{n}) &= 2i \frac{(\partial_\nu u \partial_\mu u^* - \partial_\mu u \partial_\nu u^*)}{(1 + |u|^2)^2} \\ (\partial_\mu \vec{n} \cdot \partial^\mu \vec{n}) &= 4 \frac{\partial_\mu u \partial^\mu u^*}{(1 + |u|^2)^2} \end{aligned} \quad (4)$$

Therefore, in terms of the field u the Lagrangian (1) reads

$$\mathcal{L} = 4M^2 \frac{\partial_\mu u \partial^\mu u^*}{(1 + |u|^2)^2} + \frac{8}{e^2} \left[\frac{(\partial_\mu u)^2 (\partial_\nu u^*)^2}{(1 + |u|^2)^4} + (\beta e^2 - 1) \frac{(\partial_\mu u \partial^\mu u^*)^2}{(1 + |u|^2)^4} \right] \quad (5)$$

The same static Hamiltonian (2) is now written as

$$\mathcal{H}_{\text{static}} = 4M^2 \frac{\partial_i u \partial_i u^*}{(1 + |u|^2)^2} - \frac{8}{e^2} \left[\frac{(\partial_i u)^2 (\partial_j u^*)^2}{(1 + |u|^2)^4} + (\beta e^2 - 1) \frac{(\partial_i u \partial_i u^*)^2}{(1 + |u|^2)^4} \right] \quad (6)$$

Therefore, it is positive definite for

$$M^2 > 0; \quad e^2 < 0; \quad \beta < 0; \quad \beta e^2 \geq 1 \quad (7)$$

It is that sector that we shall consider in this paper. We show that it possesses static soliton solutions with non-trivial Hopf topological charge. If one compares (1) with the effective Lagrangian given by eq. (14) or (21) of [21] one observes that, in order for them to agree, e^2 and β should indeed have the same sign. In the physical limit where the infrared cutoff goes to zero it follows that they both become positive, contrary to our assumption. However, the perturbative calculations in [21] are not valid in that limit, and so not much can be said even about their relative signs. An interesting study of such sector was performed in [24] with an additional term in the action containing second derivatives of the \vec{n} field and corresponding to the extra term obtained in [21] when the hard modes of \vec{n} are also integrated out.

Another interesting aspect of the theory (1) has to do with its integrability properties. The Euler-Lagrange equations following from (5), or equivalently (1), reads

$$(1 + |u|^2) \partial^\mu \mathcal{K}_\mu - 2u^* \mathcal{K}_\mu \partial^\mu u = 0 \quad (8)$$

together with its complex conjugate, and where

$$\mathcal{K}_\mu \equiv M^2 \partial_\mu u + \frac{4}{e^2} \frac{[(\beta e^2 - 1) (\partial_\nu u \partial^\nu u^*) \partial_\mu u + (\partial_\nu u \partial^\nu u) \partial_\mu u^*]}{(1 + |u|^2)^2} \quad (9)$$

The theory (1) has three conserved currents associated the $O(3)$ internal symmetry. However, using the techniques of [25, 26] one can show that the sub-sector defined by the constraint

$$\partial_\mu u \partial^\mu u = 0 \quad (10)$$

possesses an infinite number of conserved currents given by

$$J_\mu \equiv \frac{\delta G}{\delta u} \mathcal{K}_\mu^c - \frac{\delta G}{\delta u^*} \mathcal{K}_\mu^{c*} \quad (11)$$

where G is any function of u and u^* , but not of their derivatives, and \mathcal{K}_μ^c is obtained from (9) by imposing (10), i.e.

$$\mathcal{K}_\mu^c \equiv M^2 \partial_\mu u + \frac{4}{e^2} \frac{(\beta e^2 - 1) (\partial_\nu u \partial^\nu u^*) \partial_\mu u}{(1 + |u|^2)^2} \quad (12)$$

The fact that currents (11) are conserved follows from the identity $Im(\mathcal{K}_\mu \partial^\mu u^*) = 0$, the condition $\mathcal{K}_\mu^c \partial^\mu u = 0$ following from (10), and the equations of motion, which now read $\partial^\mu \mathcal{K}_\mu^c = 0$.

If in addition of (10) one restricts to the sector where the coupling constants satisfy

$$\beta e^2 = 1 \quad (13)$$

then the equations of motion simplify to $\partial^2 u = 0$, and the theory becomes scaling invariant. That constitutes an integrable sub-sector of the theory (1). Exact vortex solutions were constructed in [27], using quite simple and direct methods. One can have multi-vortex solutions all lying in the same direction, and the vortices can be either static or have waves traveling along them with the speed of light.

Apparently the integrable sub-sector defined by conditions (10) and (13) do not admit soliton solutions with non-trivial Hopf topological charges. In this paper we construct such solitons for the theory (1) in the range of the coupling constants defined in (7) and without imposing the constraint (10). We construct static solutions with axial symmetry by solving numerically the equations of motion. Due to the axial symmetry we have to solve two coupled non-linear partial differential equations in two dimensions. We choose to use the toroidal coordinates defined as

$$\begin{aligned} x^1 &= \frac{r_0}{p} \sqrt{z} \cos \varphi \\ x^2 &= \frac{r_0}{p} \sqrt{z} \sin \varphi \\ x^3 &= \frac{r_0}{p} \sqrt{1-z} \sin \xi \end{aligned} \quad p = 1 - \cos \xi \sqrt{1-z} \quad (14)$$

where x^i , $i = 1, 2, 3$, are the Cartesian coordinates in \mathbb{R}^3 , and (z, ξ, φ) are the toroidal coordinates. We have $0 \leq z \leq 1$, $-\pi \leq \xi \leq \pi$, $0 \leq \varphi \leq 2\pi$, and r_0 is a free parameter with dimension of length. Notice that the usual toroidal coordinates have a coordinate $\eta > 0$ which is related to our z by $z = \tanh^2 \eta$.

We construct solutions which are invariant under the diagonal $U(1)$ subgroup of the direct product of the $U(1)$ group of rotations on the $x^1 x^2$ plane and the $U(1)$ group of internal phase transformations $u \rightarrow e^{i\alpha} u$. We then use the ansatz

$$u = \sqrt{\frac{1-g(z, \xi)}{g(z, \xi)}} e^{i\Theta(z, \xi) + i n \varphi} \quad (15)$$

with n being an integer, and $0 \leq g \leq 1$, $-\pi \leq \Theta \leq \pi$.

By rescaling the Cartesian coordinates as $x^i \rightarrow x^i/r_0$, it is then clear that the equations of motion (8) will depend only upon two dimensionless parameters, namely $\beta e^2 \geq 1$ and

$$a^2 = -e^2 r_0^2 M^2 > 0 \quad (16)$$

since we are assuming (7). In addition, from (6) the static energy can be written as

$$E = \int d^3 x \mathcal{H}_{\text{static}} = \frac{4M}{|e|} \left[E_2 + 2 \left(E_4^{(1)} + (\beta e^2 - 1) E_4^{(2)} \right) \right] \quad (17)$$

in terms of the dimensionless quantities

$$\begin{aligned}
E_2 &= M |e| \int d^3x \frac{\partial_{x^i} u \partial_{x^i} u^*}{(1 + |u|^2)^2} \\
E_4^{(1)} &= \frac{1}{M |e|} \int d^3x \frac{|\partial_{x^i} u|^2}{(1 + |u|^2)^4} \\
E_4^{(2)} &= \frac{1}{M |e|} \int d^3x \frac{(\partial_{x^i} u \partial_{x^i} u^*)^2}{(1 + |u|^2)^4}
\end{aligned} \tag{18}$$

By replacing the ansatz (15) into the equations of motion (8) we get two non-linear partial differential equations for the function $g(z, \xi)$ and $\Theta(z, \xi)$, depending upon the dimensionless parameters βe^2 and a . We solve those equations numerically using a standard relaxation method [28], with appropriate boundary conditions explained below. Derrick's argument [29] implies that the contribution to the energy from the quadratic and quartic terms must equal, i.e. $E_2 = 2 \left(E_4^{(1)} + (\beta e^2 - 1) E_4^{(2)} \right)$ (see (17)). That fixes the size of the solution and so the value of a . Therefore, in our numerical procedure we determine a on each step of the relaxation method using Derrick's argument. Our main results are the following. We find finite energy axially symmetric solutions with Hopf charges up to four. The axial symmetry comes from the use of the ansatz (15). Therefore, our solutions are not necessarily the ones with the lowest possible energy for a given value of the Hopf charge. For the Skyrme-Faddeev model the solutions with Hopf charge 1 and 2 do present axial symmetry [4, 5, 6, 7, 8]. We believe the same may happen in the extended model (1). An interesting discovery we made is that $a \rightarrow 0$ as $\beta e^2 \rightarrow 1$. That means that the solutions shrink in that limit, and disappear for $\beta e^2 = 1$. In addition, the energy also vanishes in the limit $\beta e^2 \rightarrow 1$. Since all three terms in the energy (17) are positive they each vanish in that limit, including $E_4^{(2)}$, despite the factor $(\beta e^2 - 1)$ in front of it. Another interesting discovery is that $E_4^{(1)}$ is very small compared to the other two terms. In fact, for a wide range of the parameter βe^2 we have

$$\frac{E_4^{(1)}}{E_2 + 2 \left(E_4^{(1)} + (\beta e^2 - 1) E_4^{(2)} \right)} \sim 10^{-3}$$

Notice that $E_4^{(1)}$ is a good measure of how close the solutions are of satisfying the constraint (10). Therefore our solutions are very close of belonging to the integrable sector possessing the infinite number of conserved currents given by (11). It would be very interesting to perform calculations with a finer mesh to improve the precision of that ratio. One thing is clear however, the closer is βe^2 to unity the better the constraint is satisfied by the solutions. However, the solutions shrink in that limit. The Hopfions then disappear and seem to give place to the vortex solutions constructed in [27]. That point certainly deserves further studies. It would be very desirable to perform simulations to see how the vortices of [27] behave when the conditions (10) and (13) are relaxed, and that fact is now under investigation.

The paper is organized as follows: in section II we calculate the Hopf topological charges for the configurations within the ansatz (15), in section III we calculate a bound for the static energy (17) using methods similar to those of references [32, 33] employed in case of the Skyrme-Faddeev model. The equations of motion in terms of the ansatz functions $g(z, \xi)$ and $\Theta(z, \xi)$ are calculated in section IV, and in section V we analyze the properties of the solutions in three limiting cases, at spatial infinity, at the circle $x_1^2 + x_2^2 = r_0^2$, with $x_3 = 0$, and also at the x^3 -axis. The numerical methods and solutions are described in section VI.

II. THE HOPF TOPOLOGICAL CHARGE

The static solutions of the theory (1) define maps from the three dimensional space \mathbb{R}^3 to the target space S^2 . In order to have finite energy solutions we need the fields to go to a vacuum configuration at spatial infinity, and so we need $\vec{n} \rightarrow \text{constant}$ for $r \rightarrow \infty$, with r being the distance to the origin of the coordinate system. Therefore, finite energy solutions map all points at spatial infinity to a fixed point of S^2 . Consequently, as far as the topological properties of such maps are concerned we can identify the points at infinity and consider the space to be S^3 instead of \mathbb{R}^3 . Then the finite energy solutions define maps $S^3 \rightarrow S^2$, and those are classified into homotopy classes labeled by an integer Q_H called the Hopf index. Such index can be calculated through an integral formula as follows [30, 31]. We first consider the mapping of the three dimensional space \mathbb{R}^3 into a 3-sphere S_Z^3 , parametrized by two complex numbers Z_k , $k = 1, 2$, such that $|Z_1|^2 + |Z_2|^2 = 1$. Using the ansatz (15) we choose such map to be given by

$$\mathbb{R}^3 \rightarrow S_Z^3 : \quad Z_1 = \sqrt{1-g} e^{i\Theta} \quad Z_2 = \sqrt{g} e^{-in\varphi} \tag{19}$$

We then map such 3-sphere into the target S^2 by

$$S^3_Z \rightarrow S^2 : \quad u = \frac{Z_1}{Z_2} \quad (20)$$

In fact, the mapping of the plane parametrized by the complex field u into the S^2 , parametrized by the triplet of scalar fields \vec{n} , is given by the stereographic projection defined in (3). The Hopf index of such map is given by [30]

$$Q_H = \frac{1}{4\pi^2} \int d^3x \vec{A} \cdot (\vec{\nabla} \wedge \vec{A}) \quad (21)$$

with

$$\vec{A} = \frac{i}{2} \sum_{k=1}^2 \left[Z_k^* \vec{\nabla} Z_k - Z_k \vec{\nabla} Z_k^* \right] \quad (22)$$

and where the integral is over the coordinates x^i of the three dimensional space \mathbb{R}^3 . Even though \vec{A} cannot be written locally in terms of u or \vec{n} , its curvature can. Indeed, from (4), (20) and (22) we have

$$F_{ij} \equiv \partial_i A_j - \partial_j A_i = \frac{1}{2} \vec{n} \cdot (\partial_i \vec{n} \wedge \partial_j \vec{n}) = i \frac{(\partial_j u \partial_i u^* - \partial_i u \partial_j u^*)}{(1 + |u|^2)^2} \quad (23)$$

Therefore the Hopf index (21) can alternatively be written as

$$Q_H = \frac{1}{8\pi^2} \int d^3x \varepsilon_{ijk} A_i F_{jk} \quad (24)$$

Performing the calculation using the toroidal coordinates (14) we find that

$$\vec{A} = \frac{p}{r_0} \left[-2 \sqrt{z(1-z)} (1-g) \partial_z \Theta \vec{e}_z - \frac{(1-g)}{\sqrt{1-z}} \partial_\xi \Theta \vec{e}_\xi + n \frac{g}{\sqrt{z}} \vec{e}_\varphi \right] \quad (25)$$

where \vec{e}_z , \vec{e}_ξ and \vec{e}_φ are the unit vectors in the direction of the changes of the position vector \vec{r} under variations of coordinates, i.e. $\vec{e}_z = \partial_z \vec{r} / |\partial_z \vec{r}|$, and so on. The metric and volume element in toroidal coordinates (14) are

$$ds^2 = \left(\frac{r_0}{p} \right)^2 \left[\frac{dz^2}{4z(1-z)} + (1-z) d\xi^2 + z d\varphi^2 \right] \quad d^3x = \frac{1}{2} \left(\frac{r_0}{p} \right)^3 dz d\xi d\varphi \quad (26)$$

Therefore the Hopf index (21) for the field configurations in the ansatz (15) is given by

$$Q_H = \frac{n}{2\pi} \int_0^1 dz \int_{-\pi}^{\pi} d\xi [\partial_z (g \partial_\xi \Theta) - \partial_\xi (g \partial_z \Theta)] \quad (27)$$

We now impose the boundary conditions

$$g(z=0, \xi) = 0 \quad g(z=1, \xi) = 1 \quad \text{for} \quad -\pi \leq \xi \leq \pi \quad (28)$$

and

$$\Theta(z, \xi = -\pi) = -m\pi \quad \Theta(z, \xi = \pi) = m\pi \quad \text{for} \quad 0 \leq z \leq 1 \quad (29)$$

with m being an integer. It then follows that $\partial_z \Theta|_{\xi=-\pi} = \partial_z \Theta|_{\xi=\pi} = 0$, and so from (27)

$$Q_H = mn \quad (30)$$

III. THE ENERGY BOUND

The static energy of the theory (1) in the regime (7) satisfy an energy bound very similar to that one found by Vakulenko and Kapitanskii [32] for the Skyrme-Faddeev model. The arguments are quite simple, and we start by the definition of F_{ij} in (23) which implies that

$$F_{ij}^2 = 2 \frac{(\partial_i u \partial_i u^*)^2}{(1 + |u|^2)^4} - 2 \frac{|(\partial_i u)^2|^2}{(1 + |u|^2)^4} \quad (31)$$

and so

$$\frac{\partial_i u \partial_i u^*}{(1 + |u|^2)^2} \geq \sqrt{\frac{F_{ij}^2}{2}} \quad (32)$$

We now rewrite the static energy density (6) as

$$\mathcal{H}_{\text{static}} = 4M^2 \frac{\partial_i u \partial_i u^*}{(1 + |u|^2)^2} - \frac{4}{e^2} (\beta e^2 - 1) F_{ij}^2 - 8\beta \frac{|(\partial_i u)^2|^2}{(1 + |u|^2)^4} \quad (33)$$

Therefore, using (32) and working in the regime (7) one has

$$\mathcal{H}_{\text{static}} \geq 4M^2 \sqrt{\frac{F_{ij}^2}{2}} - \frac{4}{e^2} (\beta e^2 - 1) F_{ij}^2 \quad (34)$$

Notice that the bounds (32) and (34) are saturated by those configurations satisfying the constraint (10). Therefore we should expect the solutions to be driven in the direction of satisfying that constraint, and that is what we find in our numerical simulations.

The static energy (17) should then satisfy (assuming the regime (7))

$$E \geq 2^{11/4} \frac{M}{|e|} \sqrt{\beta e^2 - 1} \left(\int d^3x \sqrt{F_{ij}^2} \right)^{1/2} \left(\int d^3x F_{ij}^2 \right)^{1/2} + \left[\frac{2M}{2^{1/4}} \left(\int d^3x \sqrt{F_{ij}^2} \right)^{1/2} - \frac{2}{|e|} \sqrt{\beta e^2 - 1} \left(\int d^3x F_{ij}^2 \right)^{1/2} \right]^2$$

We now use the Sobolev-type inequality [32, 33]

$$\left(\int d^3x \sqrt{F_{ij}^2} \right) \left(\int d^3x F_{ij}^2 \right) \geq \frac{1}{C} \left(\frac{1}{8\pi^2} \int d^3x \varepsilon_{ijk} A_i F_{jk} \right)^{3/2} \quad (35)$$

where C is a universal constant. We then get the energy bound

$$E \geq \frac{2^{11/4}}{C^{1/2}} \frac{M}{|e|} \sqrt{\beta e^2 - 1} Q_H^{3/4}$$

where we have used (24). The value of C found in [33, 34] is

$$\frac{1}{C} = 8 \cdot 3^{3/4} \sqrt{2} \pi^4$$

However, Ward in [33] conjectures that a better value is

$$\frac{1}{C} = 64 \sqrt{2} \pi^4 \quad (36)$$

Taking Ward's value (36) one then gets the bound

$$E \geq 64 \pi^2 \frac{M}{|e|} \sqrt{\beta e^2 - 1} Q_H^{3/4} \quad (37)$$

Notice that one should expect a decrease in the energy of the hopfions as βe^2 approaches unity, and that is exactly what we find in our numerical calculations.

IV. THE EQUATIONS OF MOTION

By replacing the ansatz (15) into the equations of motion (8) we get two partial non-linear differential equations for the functions $g(z, \xi)$ and $\Theta(z, \xi)$. They are given by

$$g(1-g) \left[4(z(1-z))^2 (p\partial_z R_z - R_z \partial_z p) + z(p\partial_\xi R_\xi - R_\xi \partial_\xi p) \right] \\ - (1-2g)p \left[\frac{3}{2} \left(4(z(1-z))^2 R_z \partial_z g + z R_\xi \partial_\xi g \right) - g(1-g) \left(4(z(1-z))^2 S_z \partial_z \Theta + z S_\xi \partial_\xi \Theta + (1-z) S_\varphi n \right) \right] = 0 \quad (38)$$

and

$$g(1-g) \left[4(z(1-z))^2 (p\partial_z S_z - S_z \partial_z p) + z(p\partial_\xi S_\xi - S_\xi \partial_\xi p) \right] \\ - (1-2g)p \left[\frac{3}{2} \left(4(z(1-z))^2 S_z \partial_z g + z S_\xi \partial_\xi g \right) + g(1-g) \left(4(z(1-z))^2 R_z \partial_z \Theta + z R_\xi \partial_\xi \Theta + (1-z) R_\varphi n \right) \right] = 0 \quad (39)$$

with p being defined in (14) and where

$$R_z := -\frac{1}{2} \left(g(1-g)z(1-z) + \alpha(v_a - v_b) + \gamma(v_a + v_b) \right) \partial_z g - \alpha g(1-g)v_c \partial_z \Theta \\ R_\xi := -\frac{1}{2} \left(g(1-g)z(1-z) + \alpha(v_a - v_b) + \gamma(v_a + v_b) \right) \partial_\xi g - \alpha g(1-g)v_c \partial_\xi \Theta \\ R_\varphi := -\alpha g(1-g)v_c n \\ S_z := g(1-g) \left(g(1-g)z(1-z) - \alpha(v_a - v_b) + \gamma(v_a + v_b) \right) \partial_z \Theta + \frac{1}{2} \alpha v_c \partial_z g \\ S_\xi := g(1-g) \left(g(1-g)z(1-z) - \alpha(v_a - v_b) + \gamma(v_a + v_b) \right) \partial_\xi \Theta + \frac{1}{2} \alpha v_c \partial_\xi g \\ S_\varphi := ng(1-g) \left(g(1-g)z(1-z) - \alpha(v_a - v_b) + \gamma(v_a + v_b) \right)$$

where

$$\alpha := 4 \frac{p^2}{a^2} \qquad \gamma := 4 \frac{p^2}{a^2} (\beta e^2 - 1) \quad (40)$$

and

$$v_a := \frac{1}{4} \left(4(z(1-z))^2 (\partial_z g)^2 + z(\partial_\xi g)^2 \right) \\ v_b := (g(1-g))^2 \left(4(z(1-z))^2 (\partial_z \Theta)^2 + z(\partial_\xi \Theta)^2 + (1-z)n^2 \right) \\ v_c := g(1-g) \left(4(z(1-z))^2 (\partial_z g)(\partial_z \Theta) + z(\partial_\xi g)(\partial_\xi \Theta) \right) \quad (41)$$

Besides the boundary conditions (28) and (29) leading to the Hopf index given by (30), we impose as well the additional boundary conditions

$$\partial_\xi g(z, \xi)|_{\xi=-\pi} = \partial_\xi g(z, \xi)|_{\xi=\pi} = 0, \qquad \text{for } 0 \leq z \leq 1 \quad (42)$$

$$\partial_z \Theta(z, \xi)|_{z=0} = \partial_z \Theta(z, \xi)|_{z=1} = 0, \qquad \text{for } -\pi \leq \xi \leq \pi \quad (43)$$

Notice that the equations of motion (38) and (39) are invariant under the transformations

$$\xi \leftrightarrow -\xi \qquad g(z, \xi) \leftrightarrow g(z, -\xi) \qquad \Theta(z, \xi) \leftrightarrow -\Theta(z, -\xi) \quad (44)$$

Therefore, we choose the boundary conditions

$$\partial_\xi g(z, \xi)|_{\xi=0} = 0, \qquad \Theta(z, \xi=0) = 0 \quad (45)$$

and perform our numerical calculations on the half-plane defined by $0 \leq z \leq 1$ and $0 \leq \xi \leq \pi$. The functions on the other half-plane, namely $0 \leq z \leq 1$ and $-\pi \leq \xi \leq 0$, are obtained from the symmetry (44).

V. THE BEHAVIOR OF THE SOLUTIONS IN LIMITING CASES

The solutions within the ansatz (15) have axial symmetry around the x^3 -axis. In addition, from (3) and (15) one observes that the condition $n_3 = \text{constant}$ implies $g = \text{constant}$. The numerical solutions satisfying the boundary conditions (28), (29), (42), (43) and (45), that we find are such that for a given value of ξ , g is a monotonically increasing function of z . In addition, for a given value of z , g does not vary much under variations of ξ . It then turns out that the surfaces in \mathbb{R}^3 corresponding to constant n_3 have a toroidal shape. They are in fact deformations of the toroidal surfaces obtained by fixing z and varying ξ and φ (see (14)). It is then important to analyze the behavior of the solutions in three regions, namely the spatial infinity and close to the x^3 -axis where due to the boundary condition (28) we have $n_3 = 1$, and close to the circle on the $x^1 x^2$ -plane of radius r_0 and centered at the origin, where $n_3 = -1$. We now perform such analysis.

A. The behavior at spatial infinity

From (14) one observes that

$$r^2 \equiv x_1^2 + x_2^2 + x_3^2 = r_0^2 \frac{(1 + \sqrt{1 - z} \cos \xi)}{(1 - \sqrt{1 - z} \cos \xi)}$$

Therefore, in the toroidal coordinates (14) the limit $r \rightarrow \infty$ corresponds to the double limit $z \rightarrow 0$ and $\xi \rightarrow 0$. We choose to perform such double limit through the parametrization

$$z \sim \varepsilon_1^2 \cos^2 \sigma \quad \xi \sim \varepsilon_1 \sin \sigma \quad \text{with} \quad \varepsilon_1 \rightarrow 0 \quad 0 \leq \sigma \leq \frac{\pi}{2} \quad (46)$$

That corresponds to polar coordinates on the plane (\sqrt{z}, ξ) , and the derivatives are related by

$$\begin{aligned} \partial_z &= \frac{1}{2\varepsilon_1^2 \cos \sigma} (\varepsilon_1 \cos \sigma \partial_\varepsilon - \sin \sigma \partial_\sigma) \\ \partial_\xi &= \sin \sigma \partial_\varepsilon + \frac{\cos \sigma}{\varepsilon} \partial_\sigma \end{aligned}$$

Taking into account the boundary conditions (28), (43) and (45) we then assume the fields to behave as

$$g \sim \varepsilon_1^{s_1} f(\sigma) \quad \Theta \sim \varepsilon_1^{r_1} h(\sigma) \quad (47)$$

where s_1 and r_1 are constants, and with the test functions satisfying

$$f\left(\frac{\pi}{2}\right) = 0 \quad f'(0) = 0 \quad h(0) = 0 \quad h'\left(\frac{\pi}{2}\right) = 0 \quad (48)$$

where primes denote derivatives w.r.t. σ . Replacing the expansions (47) into the equations of motion (38) and (39), and keeping only the leading terms, i.e. those with the smallest possible power of ε_1 , we get the following equations for the test functions

$$\left(\frac{f'}{f}\right)' + \frac{1}{2} \left(\frac{f'}{f}\right)^2 - \tan \sigma \frac{f'}{f} + \frac{1}{2} s_1 (s_1 - 2) - \frac{2n^2}{\cos^2 \sigma} = 0 \quad (49)$$

and

$$\frac{h''}{h} + \left[\frac{f'}{f} - \tan \sigma\right] \frac{h'}{h} + r_1 (r_1 + s_1 - 1) = 0 \quad (50)$$

A solution of (49) satisfying the boundary conditions (48) is given by

$$f \sim (\cos \sigma)^{2|n|} \quad \text{with} \quad s_1 = 2(|n| + 1) \quad (51)$$

Replacing (51) into (50) and performing the change of variables

$$x = \sin^2 \sigma \quad 0 \leq \sigma \leq \frac{\pi}{2} \quad 0 \leq x \leq 1$$

we get that the equation (50) becomes an hypergeometric equation of the form

$$x(1-x) \partial_x^2 h + \frac{1}{2} [1 - (2|n|+3)x] \partial_x h + \frac{1}{4} r_1 (r_1 + 2|n|+1) h = 0 \quad (52)$$

The boundary conditions (48) imply that

$$h|_{x=0} = 0 \quad \partial_x h|_{x=1} = \text{finite} \quad (53)$$

There are two independent solutions for equation (52), namely

$$h_1 = F\left(|n| + \frac{r_1+1}{2}, -\frac{r_1}{2}, \frac{1}{2}, x\right)$$

$$h_2 = x^{1/2} F\left(|n| + \frac{r_1}{2} + 1, -\frac{r_1}{2} + \frac{1}{2}, \frac{3}{2}, x\right)$$

where $F(\alpha, \beta, \gamma, x)$ is the Gauss hypergeometric series. One can check that such series does not converge since in both cases we have $\alpha + \beta - \gamma = |n| \geq 1$. We then have to choose r_1 in order to truncate the series. That leads us to the allowed values for r_1

$$r_1 = 2l + 1 \quad l = 0, 1, 2, \dots$$

Since the first term of F is 1, we see that only h_2 satisfies the boundary condition (53). Therefore, the allowed solutions for Θ are

$$\Theta \sim \varepsilon_1^{2l+1} \sin \sigma F\left(|n| + l + \frac{3}{2}, -l, \frac{3}{2}, \sin^2 \sigma\right) \quad l = 0, 1, 2, \dots$$

In our numerical calculations only solutions corresponding to $l = 0$ appear (so $F = 1$), and therefore the behavior of our solutions at spatial infinity, i.e. $z, \xi \sim 0$, is given by

$$g \sim \varepsilon_1^{2(|n|+1)} (\cos \sigma)^{2|n|} \sim z^{|n|} (z + \xi^2) \quad \Theta \sim \varepsilon_1 \sin \sigma \sim \xi \quad (54)$$

That implies that the u field at spatial infinity behaves as

$$u \rightarrow \frac{1}{(2r_0)^{|n|+1}} \frac{r^{2|n|+1}}{\rho^{|n|}} e^{in\varphi} \quad (55)$$

with $\rho^2 = x_1^2 + x_2^2$, and $r^2 = x_1^2 + x_2^2 + x_3^2$. Therefore, we indeed have $\vec{n} \rightarrow (0, 0, 1)$, as $r \rightarrow \infty$.

B. The behavior around the circle $x_1^2 + x_2^2 = r_0^2$, and $x_3 = 0$

The circle $x_1^2 + x_2^2 = r_0^2$, and $x_3 = 0$ correspond to $z = 1$ and any ξ and φ , and so we write

$$\varepsilon_2 \equiv 1 - z \rightarrow 0$$

We assume the following behavior for the fields

$$g \sim 1 - \varepsilon_2^{s_2} F(\xi) \quad \Theta \sim H(\xi) - \varepsilon_2^{r_2} K(\xi) \quad (56)$$

with s_2 and r_2 being constants. The boundary conditions (29), (42), (43) and (45) impose the following conditions on the trial functions

$$\begin{aligned} \partial_\xi g|_{\xi=0, \pm\pi} = 0 &\rightarrow F'|_{\xi=0, \pm\pi} = 0 \\ \Theta|_{\xi=0} = 0 &\rightarrow H|_{\xi=0} = 0 \quad K|_{\xi=0} = 0 \\ \Theta|_{\xi=\pm\pi} = \pm m\pi &\rightarrow H|_{\xi=\pm\pi} = \pm m\pi \quad K|_{\xi=\pm\pi} = 0 \\ \partial_z \Theta|_{z=1} = 0 &\rightarrow r_2 > 1 \end{aligned} \quad (57)$$

The last condition plays an important role in our analysis. In addition, we do not want the z -derivative of g to diverge close to $z = 1$, and so we need $s_2 \geq 1$. Replacing those expansions in the equations of motion (38) and (39) and keeping only the leading terms we get

$$\begin{aligned} & \frac{1}{2} \left(\frac{F'}{F} \right)' + \frac{1}{4} \left(\frac{F'}{F} \right)^2 + s_2^2 - (H')^2 \\ & + \delta_{s_2,1} \left[\frac{1}{2} \frac{F'}{F} G'_+ + G_+ \left(\frac{1}{2} \left(\frac{F'}{F} \right)' + \frac{1}{4} \left(\frac{F'}{F} \right)^2 + 1 \right) - (H')^2 G_- + \alpha \left(F' (H')^2 \right)' \right] = 0 \end{aligned} \quad (58)$$

and

$$\frac{H''}{H'} + \frac{F'}{F} + \delta_{s_2,1} \left[\alpha F' \left[1 + (H')^2 - \frac{1}{4} \left(\frac{F'}{F} \right)^2 + \frac{F''}{F} + \frac{1}{2} \frac{F'}{F} \frac{H''}{H'} \right] + G'_- + \frac{1}{2} \frac{F'}{F} (G_+ + G_-) + \frac{H''}{H'} G_- \right] = 0 \quad (59)$$

where the primes denote derivatives w.r.t. ξ , and where $\delta_{s_2,1}$ is the Kronecker delta and so those terms only exist in the case $s_2 = 1$. In addition we have introduced the quantities

$$G_{\pm} \equiv F \left[\gamma \left(1 + \frac{1}{4} \left(\frac{F'}{F} \right)^2 + (H')^2 \right) \pm \alpha \left(1 + \frac{1}{4} \left(\frac{F'}{F} \right)^2 - (H')^2 \right) \right]$$

and α and γ are the values of the functions (40) in the limit $z \rightarrow 1$, i.e.

$$\alpha \sim \frac{4}{a^2} \quad \gamma \sim \frac{4}{a^2} (\beta e^2 - 1)$$

Notice that the function $K(\xi)$ introduced in (56) is not determined in such expansion up to leading order.

For the numerical calculations we perform, the relevant solution for equations (58) and (59), satisfying the boundary conditions (57), is

$$s_2 = |m| \quad F = \text{const.} \quad H = m \xi$$

and so

$$g \sim 1 - \text{const.} (1-z)^{|m|} \quad \Theta \sim m \xi$$

Therefore, the behavior of the u field around the circle $x_1^2 + x_2^2 = r_0^2$, and $x_3 = 0$ is

$$u \rightarrow \text{const.} (1-z)^{|m|/2} e^{i(m \xi + n \varphi)} \quad z \rightarrow 1 \quad (60)$$

Therefore we indeed have $\vec{n} \rightarrow (0, 0, -1)$ on that circle.

C. The behavior of the solutions around the x^3 -axis

From (14) we see that the x^3 -axis corresponds to $z = 0$, and any ξ and φ . Therefore we denote

$$\varepsilon_3 \equiv z \rightarrow 0$$

We assume the following behavior for the fields

$$g \sim \varepsilon_3^{s_3} \mathcal{F}(\xi) \quad \Theta \sim \mathcal{H}(\xi) + \varepsilon_3^{r_3} \mathcal{K}(\xi) \quad (61)$$

with s_3 and r_3 being constants. The boundary conditions (29), (42), (43) and (45) impose the following conditions on the trial functions

$$\begin{aligned} \partial_{\xi} g |_{\xi=0, \pm\pi} = 0 & \rightarrow \mathcal{F}' |_{\xi=0, \pm\pi} = 0 \\ \Theta |_{\xi=0} = 0 & \rightarrow \mathcal{H} |_{\xi=0} = 0 \quad \mathcal{K} |_{\xi=0} = 0 \\ \Theta |_{\xi=\pm\pi} = \pm m \pi & \rightarrow \mathcal{H} |_{\xi=\pm\pi} = \pm m \pi \quad \mathcal{K} |_{\xi=\pm\pi} = 0 \\ \partial_z \Theta |_{z=0} = 0 & \rightarrow r_3 > 1 \end{aligned}$$

The last condition will play an important role in our analysis. In addition, we do not want the z -derivative of g to diverge close to $z = 0$, and so we need $s_3 \geq 1$. Replacing those expansions into the equation of motion (38) and keeping only the leading terms we get

$$(n^2 - s_3^2) [1 + \delta_{s_3,1} \mathcal{F} \gamma (s_3^2 + n^2)] - (s_3^2 + n^2) \delta_{s_3,1} \mathcal{F} \alpha (s_3^2 - n^2) = 0 \quad (62)$$

where α and γ are the limiting values of the functions (40) in this expansion, i.e.

$$\alpha = \frac{4}{a^2} (1 - \cos \xi)^2 \quad \gamma = \frac{4}{a^2} (\beta e^2 - 1) (1 - \cos \xi)^2$$

So, apparently the only reasonable solution for (62) is

$$s_3 = |n|$$

Now replacing the same expansions in the equation of motion (39) for the cases $s_3 > r_3 > 1$ and $1 < s_3 \leq r_3$ we get the equation

$$\frac{\mathcal{H}''}{\mathcal{H}'} + \frac{\mathcal{F}'}{\mathcal{F}} - \frac{\partial_\xi p}{p} = 0 \quad s_3 > r_3 > 1 \quad 1 < s_3 \leq r_3 \quad (63)$$

and so the solution is given by $\frac{\mathcal{F} \mathcal{H}'}{p} = \text{const.}$, where p is the limiting value of the function introduced in (14), i.e.

$$p = 1 - \cos \xi$$

For the case $1 = s_3 < r_3$ the equation of motion (39) gives instead

$$(1 + 2\gamma \mathcal{F}) \frac{\mathcal{H}''}{\mathcal{H}'} + (1 + 4(\alpha + \gamma) \mathcal{F}) \frac{\mathcal{F}'}{\mathcal{F}} - (1 - 2\gamma \mathcal{F}) \frac{\partial_\xi p}{p} = 0 \quad 1 = s_3 < r_3 \quad (64)$$

We then notice that even though the function \mathcal{K} introduced in (61) does not enter into the equations, the exponent r_3 related to it does play a role in the expansion up to leading order. The difficulty of this case however is that the expansion up to leading order is not enough to determine the trial functions \mathcal{F} and \mathcal{H} separately. We would have to go to the next to leading order terms to get those functions.

VI. THE NUMERICAL ANALYSIS

The equations (38) and (39) with the boundary conditions (28), (29), (42), (43) and (45) can be solved numerically by the standard successive over-relaxation (SOR) method [28]. Such well known method is a powerful tool for finding solutions of this kind of complex set of equations. In order to find a solution f of an elliptic equation $\mathcal{L}f = \rho$ where \mathcal{L} represents some elliptic operator and ρ is the source, we rewrite it as a diffusion equation,

$$\frac{\partial u}{\partial t} = \omega(\mathcal{L}u - \rho). \quad (65)$$

The idea is that an initial distribution u relaxes to an equilibrium solution f as $t \rightarrow \infty$, and ω is called the over-relaxation parameter. (Normally one chooses $1 < \omega < 2$ for faster convergence). We apply that algorithm to our equations by putting (38), (39) into right-hand side of the diffusion equations (65). One thing we should care about is the sign of the elliptic operator. In order to get convergent solutions we found that we must choose the r.h.s. of (65) in such a way that the second derivatives of g and Θ , w.r.t. z and ξ , appear with a positive sign. Therefore, we have used the diffusion equations as

$$\frac{\partial g}{\partial t} = -\omega \mathcal{A} \quad \frac{\partial \Theta}{\partial t} = \omega \mathcal{B} \quad (66)$$

where \mathcal{A} and \mathcal{B} stand for the expressions on the l.h.s. of (38) and (39) respectively, and ω was taken to be unity in most of the simulations.

In order to estimate the derivatives in the equations, we have discretized the equations using central differences on a rectangular cubic lattice (z, ξ) . We have investigated the cases of various mesh sizes and found a good convergence for a mesh size $(N_z, N_\xi) = (80, 80)$, i.e. we divided the intervals $0 \leq z \leq 1$ and $0 \leq \xi \leq \pi$ into 80 segments each.

Q_H	(m,n)	a	E	E/E_{bound}
1	(1,1)	0.53	236.2	1.18
2	(1,2)	0.79	390.6	1.16
	(2,1)	0.66	466.7	1.39
3	(1,3)	1.09	548.7	1.21
	(3,1)	0.80	715.7	1.57
4	(1,4)	1.41	697.3	1.23
	(2,2)	0.94	765.7	1.36
	(4,1)	0.99	965.7	1.71

TABLE I: The static energy E given by (17) (in units of $\frac{M}{|e|}$) and the parameter a , defined in (16), for $\beta e^2 = 1.1$. We also compute the ratio of the energy E to the bound given in (37), i.e. $E_{\text{bound}} = 64\pi^2 \frac{M}{|e|} \sqrt{\beta e^2 - 1} Q_H^{3/4}$.

The parameter a introduced in (16) is determined by using Derrick's scaling argument. Indeed, that argument implies that the contribution to the energy coming from the quadratic and quartic terms in derivatives should equal, i.e. from (17) one has $E_2 = 2 \left(E_4^{(1)} + (\beta e^2 - 1) E_4^{(2)} \right)$. Therefore, we choose an initial value for a , and on each step of the relaxation method we determine a new value for a by imposing that condition. By using the ansatz (15) one finds that the energy (17) can be written as

$$E = \frac{4M}{|e|} \int_0^1 dz \int_{-\pi}^{\pi} d\xi \left[a \epsilon_2(z, \xi) + \frac{2}{a} \left(\epsilon_4^{(1)}(z, \xi) + (\beta e^2 - 1) \epsilon_4^{(2)}(z, \xi) \right) \right] \quad (67)$$

with a being defined in (16) and

$$\begin{aligned} \epsilon_2(z, \xi) &= \pi \frac{v_a + v_b}{pg(1-g)z(1-z)} \\ \epsilon_4^{(1)}(z, \xi) &= \pi \frac{p((v_a - v_b)^2 + v_c^2)}{(g(1-g))^2(z(1-z))^2} \\ \epsilon_4^{(2)}(z, \xi) &= \pi \frac{p((v_a + v_b)^2)}{(g(1-g))^2(z(1-z))^2} \end{aligned} \quad (68)$$

where v_a , v_b and v_c are defined in (41). Consequently, the value of a on each step of the simulation is calculated by the formula

$$a^2 = 2 \frac{\int_0^1 dz \int_{-\pi}^{\pi} d\xi \left(\epsilon_4^{(1)}(z, \xi) + (\beta e^2 - 1) \epsilon_4^{(2)}(z, \xi) \right)}{\int_0^1 dz \int_{-\pi}^{\pi} d\xi \epsilon_2(z, \xi)} \quad (69)$$

We have made several simulations studying how the solutions depend upon the integers n and m (introduced in the ansatz (15) and boundary conditions (29) respectively) and the parameter βe^2 . For the particular case of $\beta e^2 = 1.1$, we have calculated numerical solutions with Hopf topological charge up to 4. The energies as well as the size of the solutions, measured by the parameter a , are given on the Table I. We also compare the energies with the bound given by (37). Very probably the solutions with Hopf charges 3 and 4 correspond to excited states. For the Skyrme-Faddeev model the minimal energy solutions with Hopf charge $Q_H > 2$ exhibit quite complicated structures like, twists, linking loops and knots, than the simple planar tori [5, 6]. Thus, the solutions with the minimum value of energy on those sectors very probably do not have axial symmetry. The solutions corresponding to $(m, n) = (1, 1)$ and $(m, n) = (1, 2)$, and so Hopf charges 1 and 2 respectively, may correspond to the minimum of energy. That is in fact what happens in the Skyrme-Faddeev model where the solutions of charge 1 and 2 do present axial symmetry.

We have made a more detailed analysis of the solutions corresponding to $(m, n) = (1, 1)$ and $(m, n) = (1, 2)$. We have studied how those solutions depend upon the parameter βe^2 , and the results are quite interesting. The energies of those two solutions decreases as βe^2 approaches unity from above, and they vanish at $\beta e^2 = 1$. The same is true for the size of the solution. The parameter a decreases as $\beta e^2 \rightarrow 1$ and vanishes at $\beta e^2 = 1$. That means that the solutions cease to exist at that point. The results are shown in the plots of Figure 1. In addition, the contribution to the total energy from the term $E_4^{(1)}$ (see (17) and (18)) is very small for the range considered for the parameter βe^2 . It corresponds in fact to about 0.1% \sim 0.5% of the total energy (see Figure 1). From (18) we see that the term $E_4^{(1)}$

is a good measure of how close the solution is of satisfying the constraint (10), which leads to the infinite number of conserved currents (11). We see that those two solutions are very close of belonging to that integrable sector. The shrinking of the solutions can perhaps be understood by Derrick's argument. For some reason which is not very clear yet the dynamics of the theory keeps the quartic term of the energy $E_4^{(1)}$ very small. We have pointed out in section III that configurations that satisfy the constraint (10) have energies closer to the bound (37), and that may be a way of understanding why $E_4^{(1)}$ is so small. The other quartic term, namely $E_4^{(2)}$ is multiplied by $(\beta e^2 - 1)$ (see (17)) and so its contribution vanishes as $\beta e^2 \rightarrow 1$. Therefore, we are left with the quadratic term E_2 only, which cannot be balanced by the quartic terms anymore. Since that term scales as $E_2 \rightarrow \lambda E_2$, as $x^i \rightarrow \lambda x^i$, the solution tends to shrink. Another fact is that the equations of motion in the sector of the theory where $\beta e^2 = 1$, and where (10) is satisfied, present scale invariance (see comments below (7)). Therefore, if a localized solutions like the hopfions exists, then any re-scaling of it would also be a solution. But that is very improbable to happen in such a theory. Consequently, only vortex solutions like the ones constructed in [27] may exist in that sub-sector.

The solutions for the ansatz functions $g(z, \xi)$ and $\Theta(z, \xi)$ satisfying the boundary conditions (28), (29), (42), (43) and (45) are quite regular. In Figures 2 and 3 we give the plots of those functions for the cases $(m, n) = (1, 1)$ and $(m, n) = (1, 2)$ respectively, and for the values $\beta e^2 = 1.1$ and 5.0 in both cases. We show the plot in the range $0 \leq \xi \leq \pi$, and the solution in the range $-\pi \leq \xi \leq 0$, is obtained through the symmetry (44). Notice that the changes of $g(z, \xi)$ and $\Theta(z, \xi)$ under variations of βe^2 are very small. In order to visualize those changes better we also present in Figure 4 cuts of the function g at the borders $\xi = 0$ and $\xi = \pi$, and for several values of βe^2 . We also show in Figure 5 cuts of Θ at the borders $z = 0$ and $z = 1$ for several values of βe^2 .

We also present the densities of the static energy (17) in the cylindrical coordinate space ($\rho := a\sqrt{z}/p, x^3$) in Fig.6 for $Q_H = 1$, and in Fig. 7 for $Q_H = 2$, for several values of βe^2 . The following relations between two coordinates are quite useful to visualize them:

$$\xi = \pm \cos^{-1} \left[\frac{a^2 - \rho^2 - (x^3)^2}{a^4 - 2a^2(\rho^2 - (x^3)^2) + (\rho^2 + (x^3)^2)^2} \right], \quad z = \frac{4a^2\rho^2}{(a^2 + \rho^2 + (x^3)^2)^2}. \quad (70)$$

The energy density of $(m, n) = (1, 1)$ ($Q_H = 1$) solution has the lump shaped, and of the $(m, n) = (1, 2)$ ($Q_H = 2$) solution exhibits the toroidal configuration. For both case, one easily observes the shrinking of the solutions as $\beta e^2 \rightarrow 1$, and so an increase of the density around the origin.

In Fig.8, we display the energy densities for solutions with charges $Q_H > 2$. The $n = 3, 4$ solitons exhibit the toroidal shape. The radius of the tori increases as n grows. On the other hand, all $n = 1$ solitons seem to be lump shaped, however, for $m \geq 2$ they have a depression close to the origin. The size grows especially in the x^3 direction as the charge increases, and as that happens a second peak gradually emerges.

Acknowledgments L.A.F. is grateful for the hospitality at the Department of Physics of the Tokyo University of Science, and the Department of Mathematical Physics of the Toyama Prefectural University, where this work was initiated. N.S. and K. T. would like to thank the kind hospitality at Instituto de Física de São Carlos, Universidade de São Paulo. The authors acknowledge the financial support of FAPESP (Brazil). L.A.F. is partially supported by CNPq.

-
- [1] L. D. Faddeev, "Quantization of solitons", Princeton preprint IAS Print-75-QS70 (1975).
L. D. Faddeev, in it 40 Years in Mathematical Physics, (World Scientific, 1995).
- [2] T. H. R. Skyrme, "A Nonlinear field theory," Proc. Roy. Soc. Lond. A **260**, 127 (1961).
T. H. R. Skyrme, "A Unified Field Theory Of Mesons And Baryons," Nucl. Phys. **31**, 556 (1962).
J. K. Perring and T. H. R. Skyrme, "A Model unified field equation," Nucl. Phys. **31**, 550 (1962).
- [3] A.A. Belavin and A.M. Polyakov, *JETP Lett.* **22** (1975) 245-247.
- [4] L. D. Faddeev and A. J. Niemi, "Knots and particles," Nature **387**, 58 (1997) [arXiv:hep-th/9610193].
- [5] R. A. Battye and P. M. Sutcliffe, "To be or knot to be?," Phys. Rev. Lett. **81**, 4798 (1998) [arXiv:hep-th/9808129].
- [6] P. Sutcliffe, "Knots in the Skyrme-Faddeev model," Proc. Roy. Soc. Lond. A **463**, 3001 (2007) [arXiv:0705.1468 [hep-th]].
- [7] J. Hietarinta and P. Salo, "Faddeev-Hopf knots: Dynamics of linked un-knots," Phys. Lett. B **451**, 60 (1999) [arXiv:hep-th/9811053].
- [8] J. Hietarinta and P. Salo, "Ground state in the Faddeev-Skyrme model," Phys. Rev. D **62**, 081701 (2000).
- [9] J. Hietarinta, J. Jaykka and P. Salo, "Dynamics of vortices and knots in Faddeev's model", in *Workshop on Integrable Theories, Solitons and Duality (2002)*, Proceedings of Science PoS(unesp2002)017, <http://pos.sissa.it/cgi-bin/reader/conf.cgi?confid=8>
J. Hietarinta, J. Jaykka and P. Salo, "Relaxation of twisted vortices in the Faddeev-Skyrme model," Phys. Lett. A **321**

- (2004) 324 [arXiv:cond-mat/0309499].
 J. Jaykka and J. Hietarinta, “Unwinding in Hopfion vortex bunches,” arXiv:0904.1305 [hep-th].
- [10] M. Hirayama, C. G. Shi and J. Yamashita, “Elliptic solutions of the Skyrme model,” Phys. Rev. D **67**, 105009 (2003) [arXiv:hep-th/0303092];
 M. Hirayama and C. G. Shi, “A class of exact solutions of the Faddeev model,” Phys. Rev. D **69**, 045001 (2004) [arXiv:hep-th/0310042],
 C. G. Shi and M. Hirayama, “Approximate vortex solution of Faddeev model,” Int. J. Mod. Phys. A **23**, 1361 (2008) [arXiv:0712.4330 [hep-th]].
- [11] E. Babaev, L. D. Faddeev and A. J. Niemi, “Hidden symmetry and knot solitons in a charged two-condensate Bose system,” Phys. Rev. B **65**, 100512 (2002) [arXiv:cond-mat/0106152].
- [12] E. Babaev, “Knotted solitons in triplet superconductors,” Phys. Rev. Lett. **88**, 177002 (2002) [arXiv:cond-mat/0106360].
- [13] E. Babaev, “Non-Meissner electrodynamics and knotted solitons in two-component superconductors,” Phys. Rev. B **79**, 104506 (2009) [arXiv:0809.4468 [cond-mat.supr-con]].
- [14] B. A. Fayzullaev, M. M. Musakhanov, D. G. Pak and M. Siddikov, “Knot soliton in Weinberg-Salam model,” Phys. Lett. B **609**, 442 (2005) [arXiv:hep-th/0412282].
- [15] L. D. Faddeev and A. J. Niemi, Phys. Rev. Lett. **82**, 1624 (1999) [arXiv:hep-th/9807069].
- [16] Y. M. Cho, Phys. Rev. D **21**, 1080 (1980).
- [17] Y. M. Cho, Phys. Rev. D **23**, 2415 (1981).
- [18] S. V. Shabanov, Phys. Lett. B **458**, 322 (1999) [arXiv:hep-th/9903223].
- [19] L. Dittmann, T. Heinzl and A. Wipf, “A lattice study of the Faddeev-Niemi effective action,” Nucl. Phys. Proc. Suppl. **106**, 649 (2002) [arXiv:hep-lat/0110026].
 L. Dittmann, T. Heinzl and A. Wipf, “Effective theories of confinement,” Nucl. Phys. Proc. Suppl. **108**, 63 (2002) [arXiv:hep-lat/0111037].
- [20] L. D. Faddeev, “Knots as possible excitations of the quantum Yang-Mills fields,” arXiv:0805.1624.
- [21] H. Gies, “Wilsonian effective action for SU(2) Yang-Mills theory with Cho-Faddeev-Niemi-Shabanov decomposition,” Phys. Rev. D **63**, 125023 (2001), hep-th/0102026
- [22] H. Forkel, “Infrared degrees of freedom of Yang-Mills theory in the Schroedinger representation,” Phys. Rev. D **73**, 105002 (2006) [arXiv:hep-ph/0508163].
- [23] J. Gladikowski and M. Hellmund, “Static solitons with non-zero Hopf number,” Phys. Rev. D **56**, 5194 (1997) [arXiv:hep-th/9609035].
- [24] N. Sawado, N. Shiiki and S. Tanaka, “Hopf soliton solutions from low energy effective action of SU(2) Yang-Mills theory,” Mod. Phys. Lett. A **21**, 1189 (2006) [arXiv:hep-ph/0511208].
- [25] O. Alvarez, L. A. Ferreira and J. Sanchez Guillen, “A new approach to integrable theories in any dimension,” Nucl. Phys. B **529**, 689 (1998) [arXiv:hep-th/9710147].
- [26] O. Alvarez, L. A. Ferreira and J. Sanchez-Guillen, “Integrable theories and loop spaces: fundamentals, applications and new developments,” Int. J. Mod. Phys. A **24**, 1825 (2009) [arXiv:0901.1654 [hep-th]].
- [27] L. A. Ferreira, “Exact vortex solutions in an extended Skyrme-Faddeev model,” Journal of High Energy Physics JHEP05(2009)001, arXiv:0809.4303 [hep-th].
- [28] “Numerical Recipes in C: The Art of Scientific Computing”, Saul A. Teukolsky, William H. Press, William T. Vetterling (Cambridge University Press, UK, 1988). <http://www.nr.com/oldverswitcher.html>
- [29] G. H. Derrick, “Comments on nonlinear wave equations as models for elementary particles,” J. Math. Phys. **5**, 1252 (1964).
- [30] R. Bott and L. W. Tu, *Differential Forms in Algebraic Topology* (Graduate Texts in Mathematics: 82), Springer 1982.
- [31] H. Aratyn, L. A. Ferreira and A. H. Zimerman, “Exact static soliton solutions of 3+1 dimensional integrable theory with nonzero Hopf numbers,” Phys. Rev. Lett. **83**, 1723 (1999) [arXiv:hep-th/9905079]; and “Toroidal solitons in 3+1 dimensional integrable theories,” Phys. Lett. B **456**, 162 (1999), [arXiv:hep-th/9902141]
- [32] A. F. Vakulenko and L. V. Kapitanskii, “Stability Of Solitons In S^2 In The Nonlinear Sigma Model,” Sov. Phys. Dokl. **24**, 433 (1979).
- [33] R. S. Ward, “Hopf solitons on S^3 and R^3 ,” *Nonlinearity* **12**, 241-246 (1999); [arXiv:hep-th/9811176].
- [34] A. Kundu and Yu. P. Rybakov, “Closed Vortex Type Solitons With Hopf Index,” J. Phys. A **15**, 269 (1982).

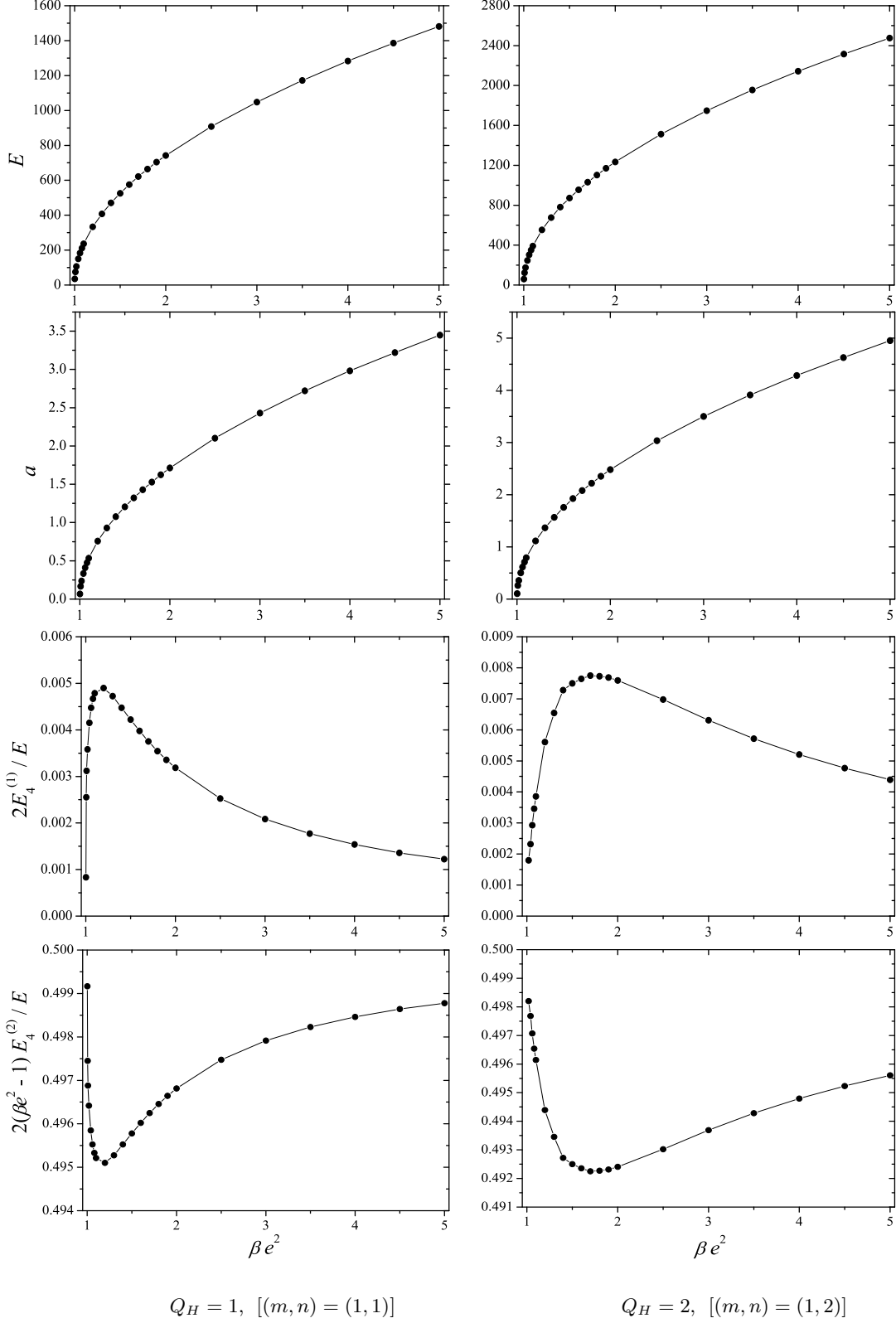


FIG. 1: The plots on the l.h.s. correspond to the solution where $(m, n) = (1, 1)$ and so Hopf charge equal to 1, and those on the r.h.s. to the solution where $(m, n) = (1, 2)$ and so Hopf charge equal to 2. On the first and second rows we plot the total energy E (see (17)) and the parameter a (see (16)) respectively, against βe^2 . On the third and fourth rows we show the fraction of the total energy corresponding to the two quartic terms, $E_4^{(1)}$ and $E_4^{(2)}$ respectively, as a function of βe^2 . Notice that due to Derrick's scaling argument we must have $E_2 = 2 \left(E_4^{(1)} + (\beta e^2 - 1) E_4^{(2)} \right)$, and so the sum of the values shown on the plots on the third and fourth rows gives 0.5.

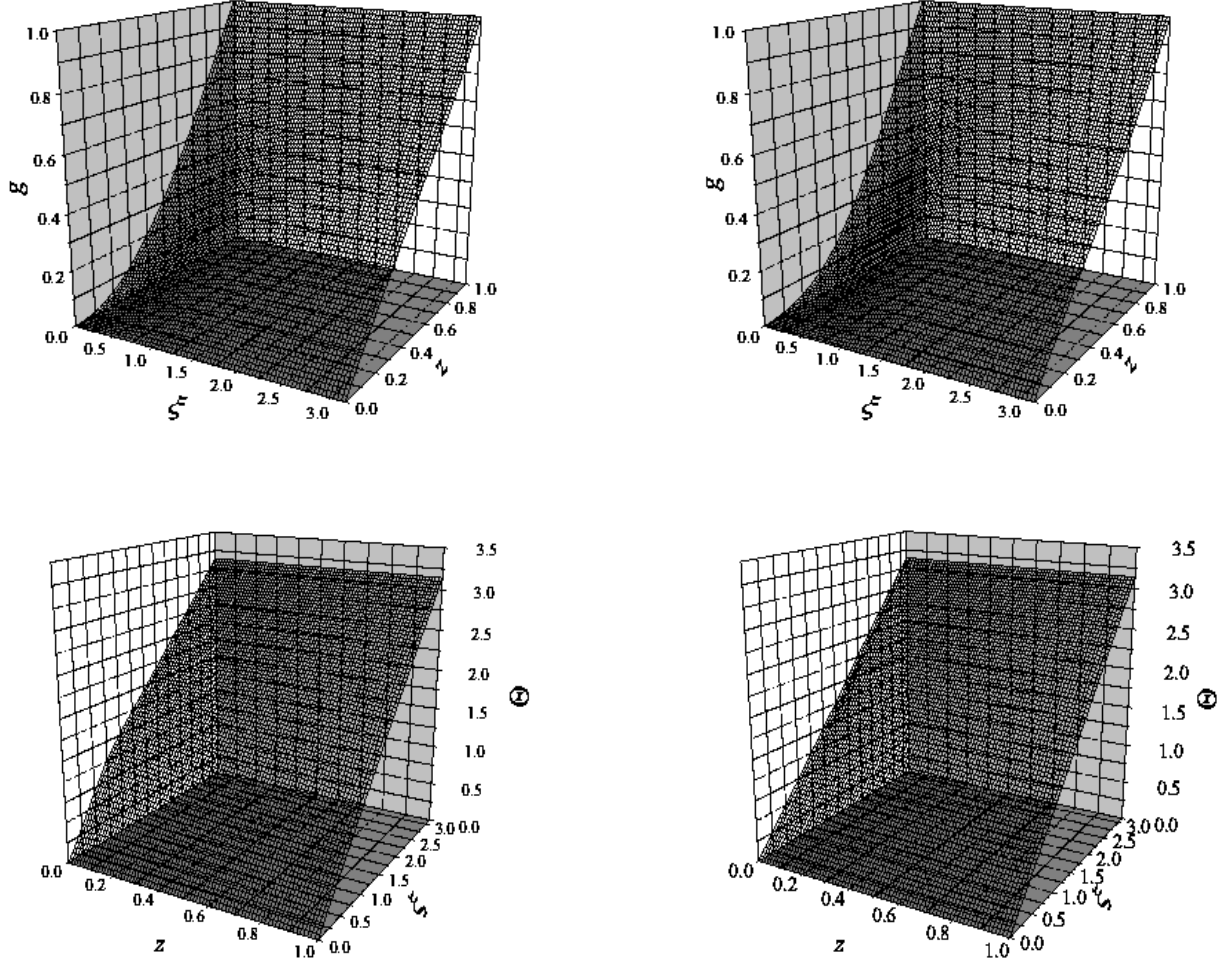


FIG. 2: The ansatz functions $g(z, \xi)$ and $\Theta(z, \xi)$ for the solution $(m, n) = (1, 1)$ ($Q_H = 1$) for $\beta e^2 = 1.1$ (left), and for $\beta e^2 = 5.0$ (right).

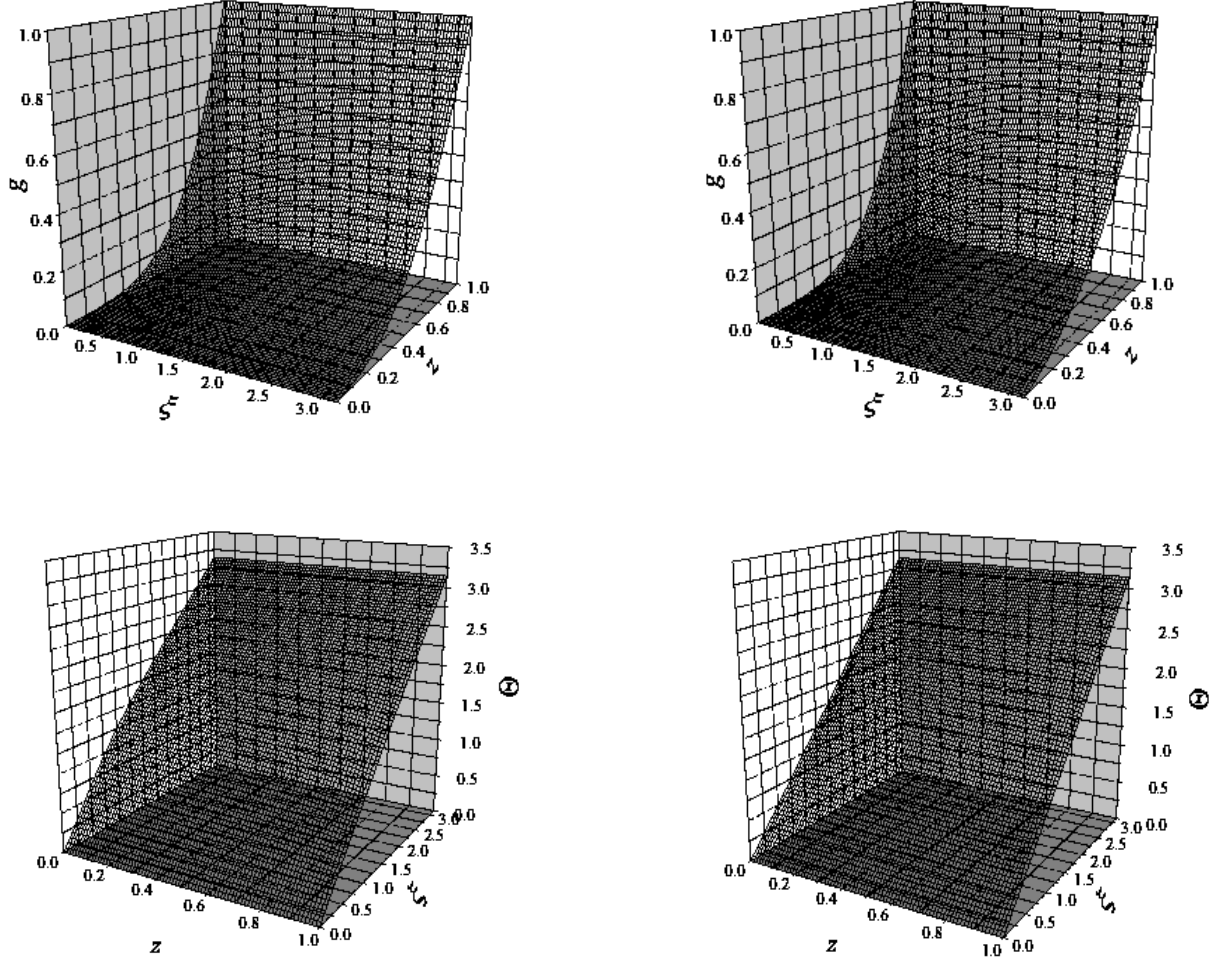
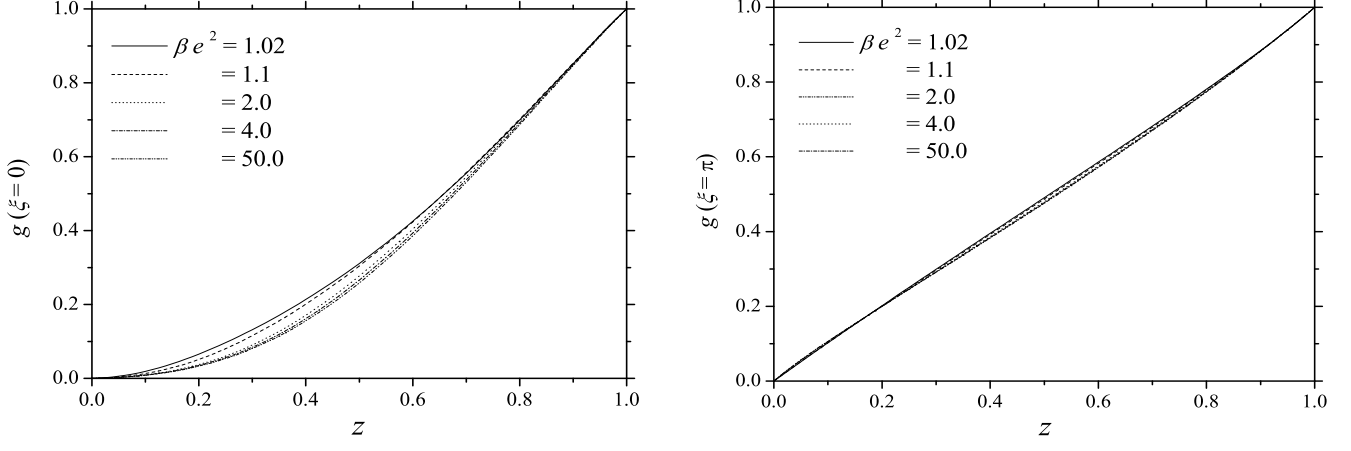
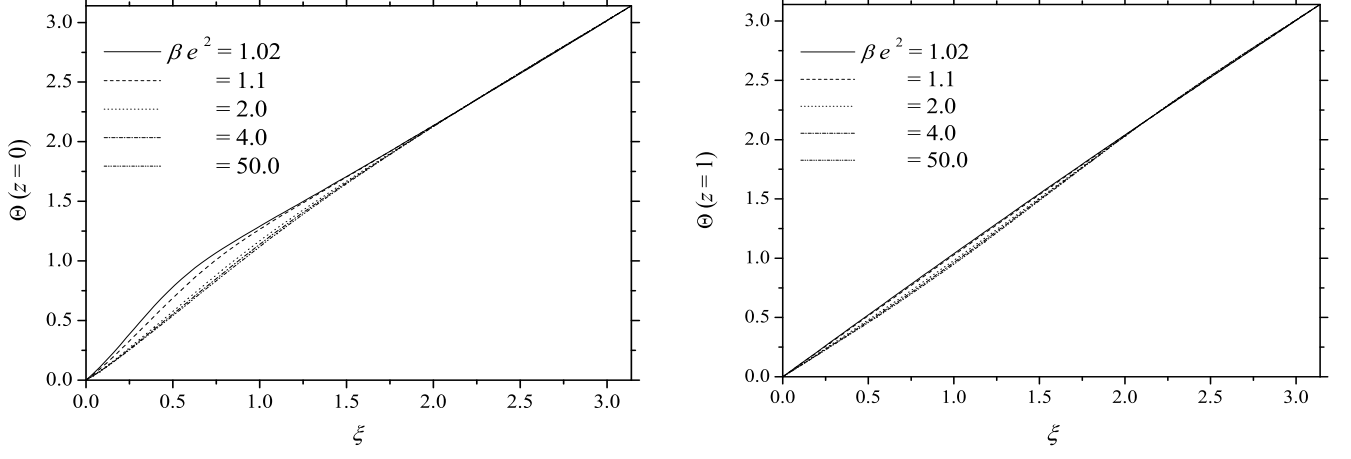


FIG. 3: The ansatz functions $g(z, \xi)$ and $\Theta(z, \xi)$ for the solution $(m, n) = (1, 2)$ ($Q_H = 2$) for $\beta e^2 = 1.1$ (left), and for $\beta e^2 = 5.0$ (right).

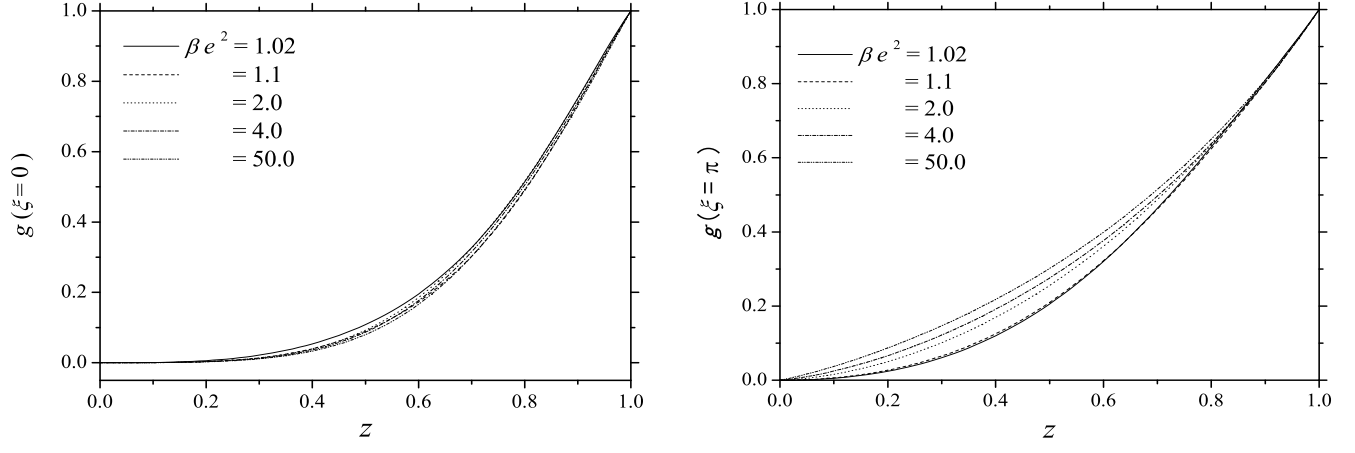


(a) $g(z, \xi)$ at $\xi = 0$ (left) and $\xi = \pi$ (right);

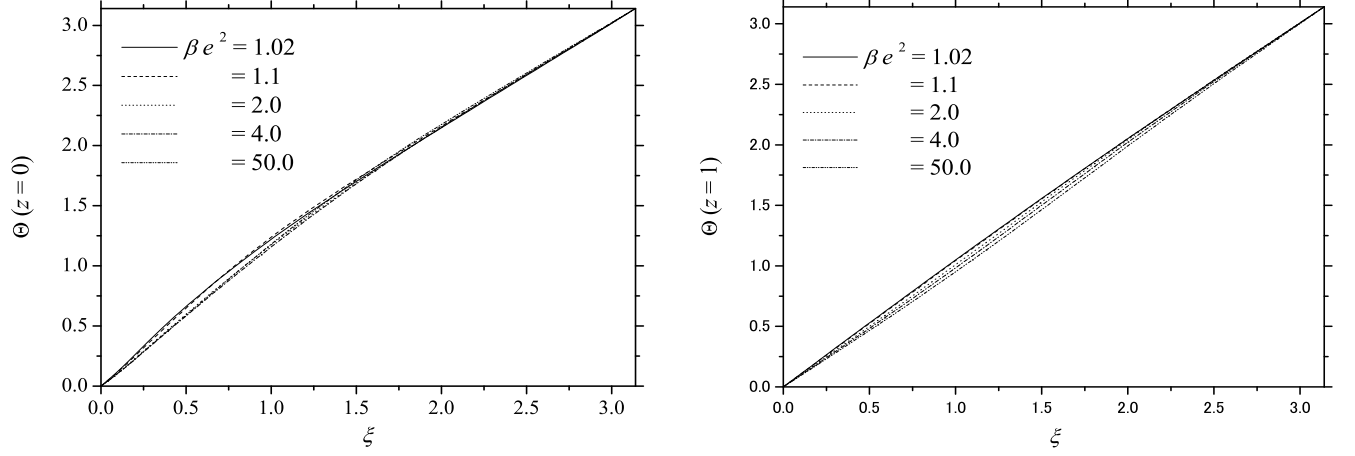


(b) $\Theta(z, \xi)$ at $z = 0$ (left) and $z = 1$ (right);

FIG. 4: Cuts of the ansatz functions $g(z, \xi)$ and $\Theta(z, \xi)$ at the boundaries for the solution $(m, n) = (1, 1)$ ($Q_H = 1$) and for some values of βe^2 shown on the plots.



(a) $g(z, \xi)$ at $\xi = 0$ (left) and $\xi = \pi$ (right);



(b) $\Theta(z, \xi)$ at $z = 0$ (left) and $z = 1$ (right);

FIG. 5: Cuts of the ansatz functions $g(z, \xi)$ and $\Theta(z, \xi)$ at the boundaries for the solution $(m, n) = (1, 2)$ ($Q_H = 2$) and for some values of βe^2 shown on the plots.

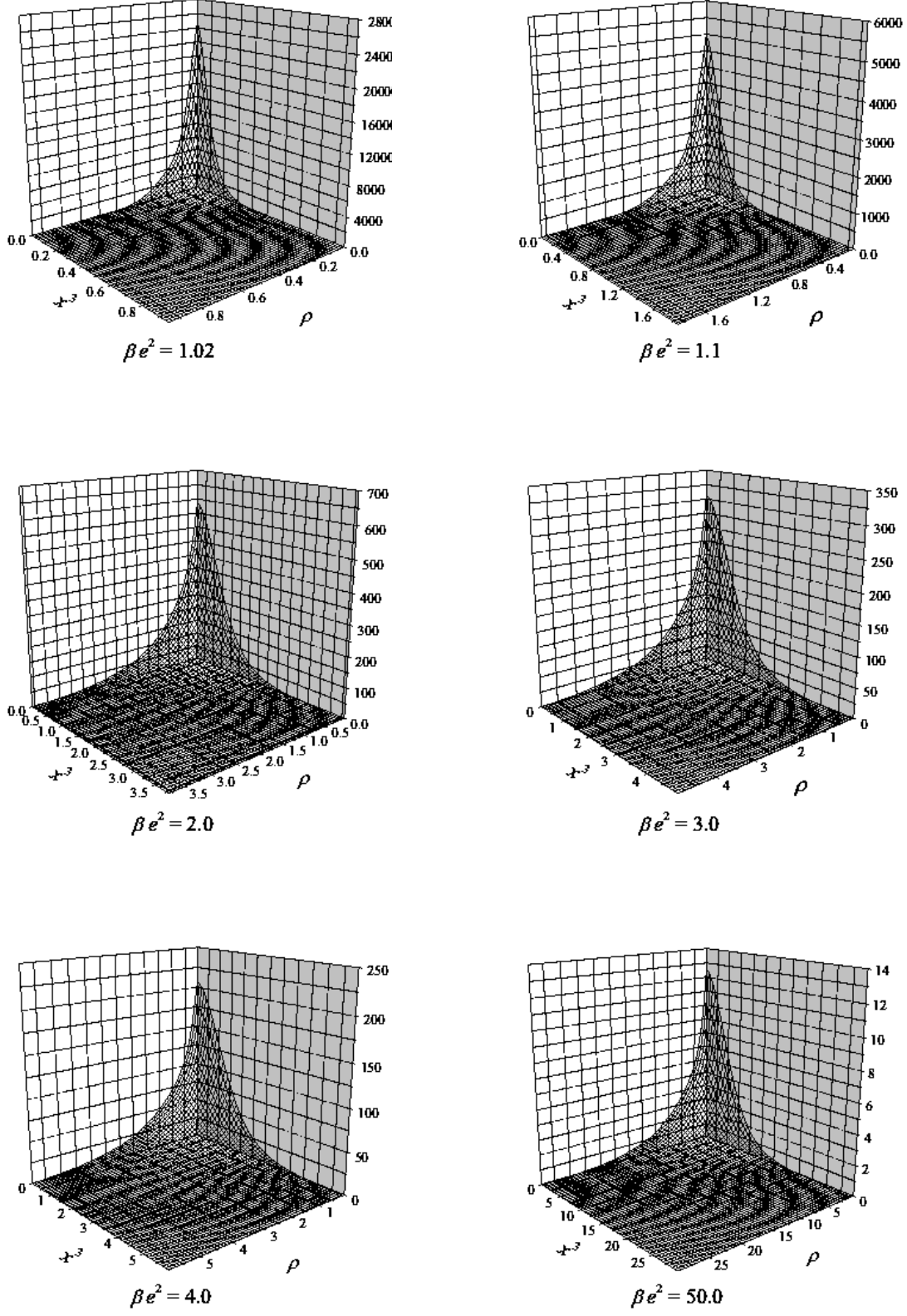


FIG. 6: The energy density (in units of $\frac{M}{|e|}$) for the solution $(m, n) = (1, 1)$ ($Q_H = 1$) on the cylindrical coordinates plane ($\rho := a\sqrt{z}/p, x^3$).

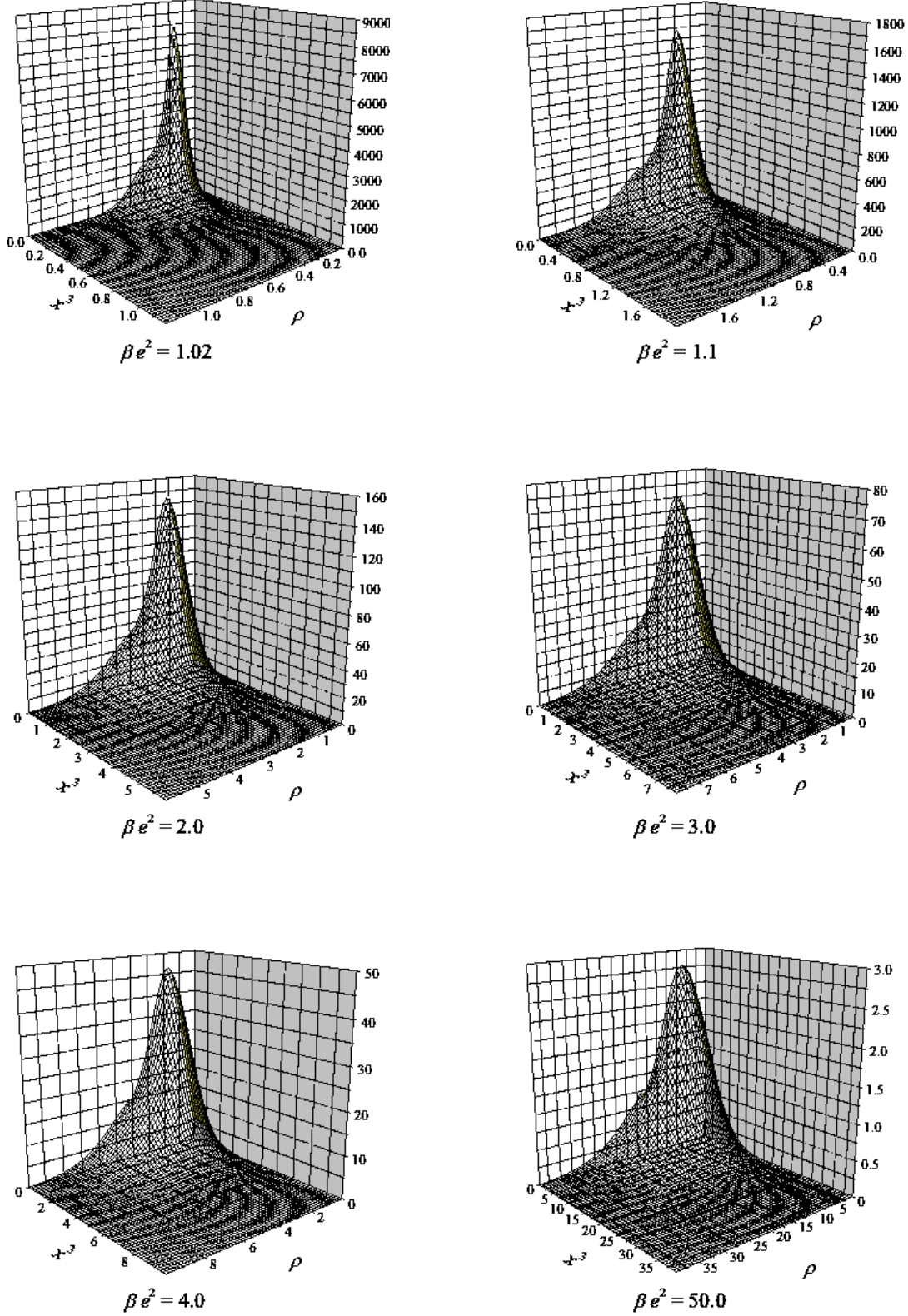


FIG. 7: The energy density (in units of $\frac{M}{|e|}$) for the solution $(m, n) = (1, 2)$ ($Q_H = 2$) on the cylindrical coordinates plane ($\rho := a\sqrt{z}/p, x^3$).

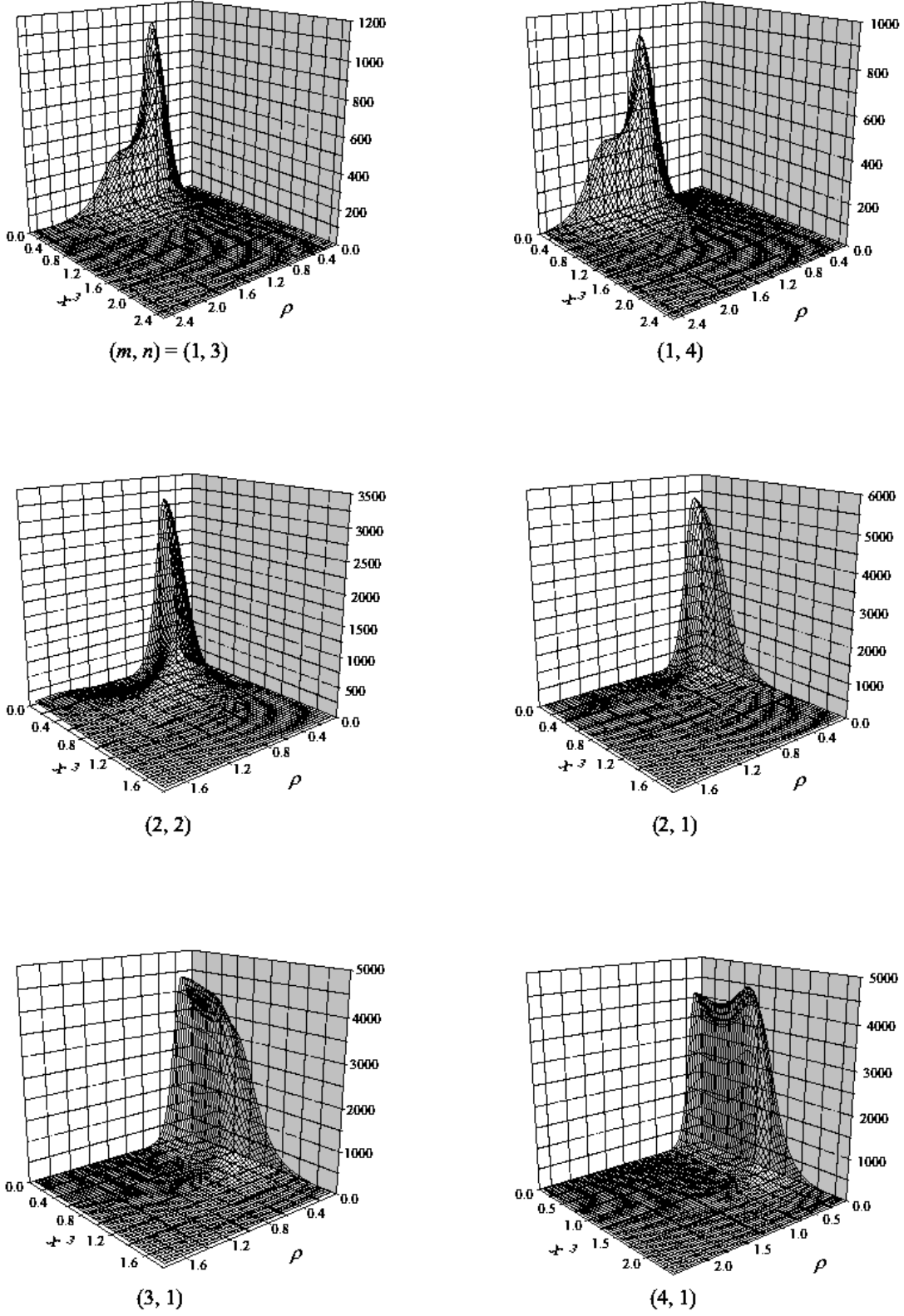


FIG. 8: The energy density (in units of $\frac{M}{|e|}$) for the solutions with higher Hopf charges $Q_H > 2$ for $\beta e^2 = 1.1$, on the cylindrical coordinates plane ($\rho := a\sqrt{z}/p, x^3$).